森脇真一	色素性乾皮症	難病事典	-	学研メディカル秀潤社（東京）	印刷中
森脇真一	UDS、ポルフィリアなど	定番・外来皮膚科検査法のすべて	-	文光堂（東京）	印刷中
森脇真一	遺伝性光線過敏症	定番・外来皮膚科検査法のすべて	-	文光堂（東京）	印刷中
森脇真一	「光や電磁波が皮膚に与える影響について教えてください。」	スキンケアマイスター試験参考テキスト（3級用）	-	メディカルレビュー社（東京）	印刷中
森脇真一	「季節、高地、緯度、湿度などで、光の曝露量が異なると、肌へどのような影響がありますか？」	スキンケアマイスター試験参考テキスト（3級用）	-	メディカルレビュー社（東京）	印刷中
森脇真一	「日焼けによって肌が赤くなり人と、黒くなる人がいますが、日焼けで違いはありますか？」	スキンケアマイスター試験参考テキスト（3級用）	-	メディカルレビュー社（東京）	印刷中
米田耕造	掌蹠角化症	平成26年度日本皮膚科学会研修講習会テキスト	日本皮膚科学会研修委員会	日本皮膚科学会（東京）	1-4, 2014

[V]
研究成果の刊行物・別刷

Immunological and Statistical Studies of Anti-BP180 Antibodies in Paraneoplastic Pemphigus

Journal of Investigative Dermatology (2014) **134,** 2283–2287; doi:10.1038/jid.2014.151; published online 24 April 2014

TO THE EDITOR

Paraneoplastic pemphigus (PNP) shows clinically intractable stomatitis and conjunctivitis with polymorphous-cutaneous lesions (Anhalt *et al.*, 1990; Hashimoto, 2001). Histopathology shows intraepidermal-acantholytic bullae and keratinocyte apoptosis (Oursler *et al.*, 1992). Most common features revealed by direct immunofluorescence (IF) are deposition of IgG to keratinocyte cell surfaces and C3 to basement membrane zone (BMZ) (Anhalt *et al.*, 1990; Hashimoto, 2001). In addition, in indirect IF, we encounter occasional reactivity with BMZ of normal skin, and more frequently with epidermal side of 1 M NaCl-split skin.

BP180 is a transmembranous collagenous protein, whose extracellular NC16a and C-terminal domains were identified as immune-dominant regions in bullous pemphigoid (BP) and mucous membrane pemphigoid, respectively (Giudice *et al.*, 1992; Matsumura *et al.*, 1996; Nie and Hashimoto, 1999; Zillikens *et al.*, 1999; Hashimoto *et al.*, 2012). Lamina lucida-type linear IgA bullous dermatosis reacts with LAD-1, truncated-extracellular domain of BP180 (Ishii *et al.*, 2008). Previous mouse model studies revealed that anti-BP180 antibodies can induce blister formation (Zillikens *et al.*, 1999), whereas the pathogenic role of BP230 is currently unclear.

Systemic study for autoantibodies to BP180 in PNP has not been performed, although a few PNP cases showed reactivity with BP180 (Preisz *et al.*, 2004). Although reactivity with BMZ in PNP may be contributed mainly by anti-BP230 antibodies, we suspected a more frequent presence of antibodies to BP180 in PNP sera.

In this study, we investigated IgG anti-BP180 antibodies in 59 PNP patients by various methods. Materials and Methods are described in Supplementary Materials online. All results of IF, immunoblotting (IB), and ELISA studies are summarized in Supplementary Table S1 online. Clinical parameters examined are shown in Supplementary Table S2 online. The results of statistical analyses are

Abbreviations: BMZ, basement membrane zone; BP, bullous pemphigoid; HaCaT, concentrated culture supernatant of HaCaT cells; IB, immunoblotting; IF, immunofluorescence; PNP, paraneoplastic pemphigus; RP, recombinant protein

Accepted article preview online 31 March 2014; published online 24 April 2014

Table 1. Results of indirect IF, IB, and ELISA and statistical analyses of sensitivity among them

(a) Results of indirect IF, IB, and ELISA

Methods	Substrates	Positive	Negative	Positive rate
IIF	Normal skin	27	32	45.80%
	Split skin	26	33	44.10%
	Normal skin and Split skin[a]	27	32	45.80%
IB	Epidermal	6	53	10.10%
	HaCaT	8	51	13.56%
	BP180 NC16a	7	52	11.86%
	BP180CT	13	46	22.03%
	BP180 NC16a and BP180CT[b]	17	42	28.81%
	all[c]	22	37	37.29%
ELISA	BP180 NC16a	17	42	28.81%
	BP180CT	9	50	15.30%
	BP180 NC16a and BP180CT[b]	24	35	40.68%

(b) Statistical analyses of sensitivity among indirect IF, IB, and ELISA

Morthods		IIF			IB						ELISA		
	Substrates	Normal skin	Split skin	Normal skin and Split skin[a]	Epidermal	HaCaT	BP180 NC16a	BP180CT	BP180 NC16a and BP180CT[b]	all[c]	BP180 NC16a	BP180CT	BP180 NC16a and BP180CT[b]
IIF	Normal skin		0.853	1	<0.001	<0.001	<0.001	0.006	0.057	0.35	0.057	<0.001	0.578
	Split skin			0.853	<0.001	<0.001	<0.001	0.011	0.085	0.453	0.085	<0.001	0.709
	Normal skin and Split skin[a]				<0.001	<0.001	<0.001	0.006	0.057	0.35	0.057	<0.001	0.578
IB	Epidermal					0.569	0.769	0.08	0.011	<0.001	0.011	0.407	<0.001
	HaCaT						0.782	0.229	0.043	0.003	0.043	0.793	<0.001
	BP180 NC16a							0.141	0.022	0.001	0.022	0.591	<0.001
	BP180CT								0.388	0.07	0.388	0.344	0.029
	BP180 NC16a and BP180CT[b]									0.328	1	0.076	0.176
	all[c]										0.328	0.006	0.706
ELISA	BP180 NC16a											0.076	0.176
	BP180CT												0.002
	BP180 NC16a and BP180CT[b]												

Abbreviations: IB, immunoblotting; IF, immunofluorescence; IIF, indirect IF.
All statistical analyses for sensitivity between two groups were done by χ^2-test. BP180 NC16a, BP180 NC16a domain RP. BP180CT, BP180 C-terminal domain RP.
Red numbers in panel b indicate statistically significant difference between positive and negative results in each analysis ($P<0.05$). Cells in panel b are categorized for combinations of statistical analyses by coloring; light green, IIF vs. IIF; light yellow, IIF vs. IB; tan, IIF vs. ELISA; light turquoise, IB vs. IB; pale blue, IB vs. ELISA; rose, ELISA vs. ELISA.
[a]IIF-positive reaction in normal-human skin only, split skin only, or both of them.
[b]IB or ELISA-positive reaction in BP180 NC16a domain RP only, BP180 C-terminal domain RP only, or both of them.
[c]IB-positive reaction in epidermal extracts only, HaCaT only, BP180 NC16a domain RP only, BP180 C-terminal domain RP only, or 2–4 of them.

Figure 1. Clinical, histopathological, and immunological features. Clinical tense blisters (**a**) and histopathological subepidermal blister (**b**). Direct immunofluorescence (IF) for IgG (**c**) and C3 (**d**). Indirect IF of human skin (**e**) and split skin (**f, g**). Scale bars = 50 μm. (**h-k**) IB results for all paraneoplastic pemphigus patients (lanes 1–59) and two normal sera (lanes N1 and N2). (**h**) Normal-human epidermal extracts. BP serum reacted with BP230 and BP180 (lane P). Black and blue asterisks, positive for BP230 and BP180, respectively. EPL, envoplakin; IB, immunoblotting; PPL, periplakin. (**i**) HaCaT. BP serum reacted with LAD-1 (lane P). Red numbers, positive. (**j**) BP180 NC16a domain RP with positive reactivity by BP serum (lane P). Red numbers, positive. (**k**) BP180 C-terminal domain RP with positive reactivity with mucous membrane pemphigoid serum (lane P). Red numbers, positive.

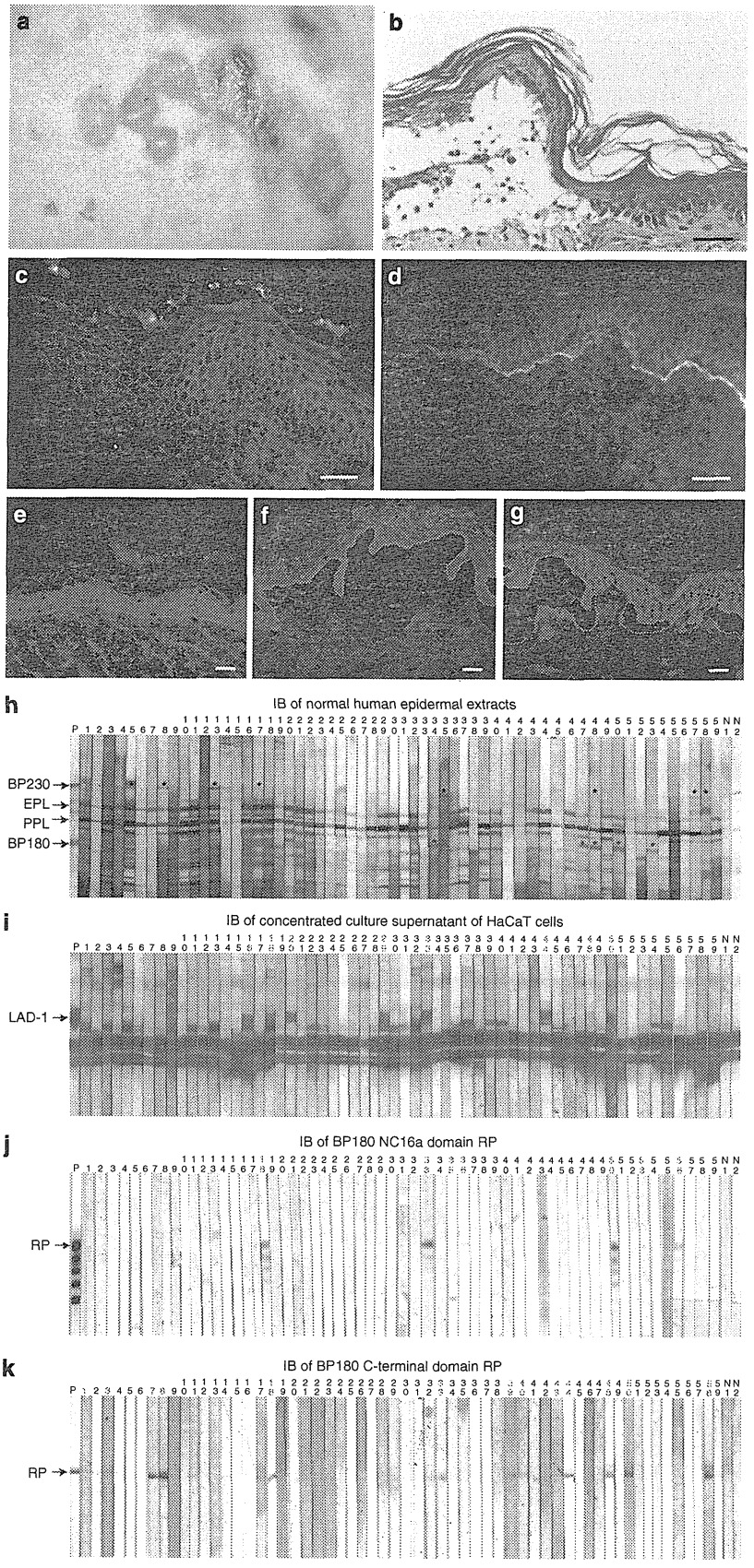
a
b
c
d
e
f
g
h
IB of normal human epidermal extracts
BP230
EPL
PPL
BP180
i
IB of concentrated culture supernatant of HaCaT cells
LAD-1
j
IB of BP180 NC16a domain RP
RP
k
IB of BP180 C-terminal domain RP
RP

summarized in Table 1 and Supplementary Table S2 online.

BP-like tense blisters were described in six PNP patients (Figure 1a). Histopathology identified apparent subepidermal blister formation in 3 of 30 skin biopsies (Figure 1b). Direct IF for 29 patients detected IgG deposition to keratinocyte cell surfaces in 21 patients (Figure 1c) and C3 deposition to BMZ in 12 patients (Figure 1d).

Indirect IF for all 59 PNP sera showed reactivity with BMZ of normal-human skin in 27 sera (Figure 1e), and reactivity with epidermal side of 1 M NaCl-split skin in 26 sera (Figure 1f). One serum reacted with both epidermal and dermal sides (Figure 1g).

In IB of normal-human epidermal extract, all 59 PNP sera reacted with both envoplakin and periplakin (Figure 1h). In addition, six sera reacted with BP180-like protein, whereas eight sera reacted with BP230-like protein (Figure 1h). IB of concentrated culture supernatant of HaCaT cells (HaCaT) showed reactivity with LAD-1-like protein in eight sera (Figure 1i). Recombinant proteins (RPs) of BP180 NC16a and C-terminal domains were detected in 7 and 13 sera, respectively (Figure 1j,k). BP sera, but not pemphigus vulgaris, pemphigus foliaceus, and normal sera, reacted with these proteins (Supplementary Figure S1 online).

In ELISA, 17 sera reacted with BP180 NC16a domain RP. Index values were 9–50 in 13 sera, 51–100 in 1 serum, and more than 101 in 3 sera. In contrast, only four sera reacted with combined RPs of BP230 N- and C-terminal domains at index values of 9–50. In newly developed ELISA for BP180 C-terminal domain RP, nine sera showed positive reactivity with OD_{450}, with values of 0.2–0.5 in four sera, 0.6–1 in four sera and more than 1 in one serum. Relatively higher reactivity with BP180 in ELISA and/or IB was shown in four of the six PNP patients with BP-like blisters, suggesting that the BP-like blisters may be caused by anti-BP180 antibodies.

Statistical analyses for the correlation between BP180 antibodies and clinical features (Supplementary Table S2a online) revealed that skin lesions on the extremities were seen significantly more frequently in PNP patients with positive reactivity with BP180 NC16a or C-terminal domain RP by ELISA or IB ($P<0.05$) (Supplementary Table S2b, c online). These results suggested that anti-BP180 autoantibodies may induce BP-like skin lesions on the trauma-prone extremities. Other clinical features, including age, gender, neoplasm, respiratory diseases, and mucocutaneous lesions, showed no significant correlation with anti-BP180 antibodies.

Statistical analyses of sensitivity among indirect IF, IB, and ELISA revealed that indirect IF of both normal-human skin and 1 M NaCl-split skin showed higher sensitivity than IB of epidermal extracts for native BP180, IB of RP of either BP180 NC16a or C-terminal domain, and IB of HaCaT for LAD-1 (Table 1a, b). This higher sensitivity of IF compared with IB may be caused by anti-BP230 antibodies, which are detected in most PNP sera by immunoprecipitation.

In contrast, sensitivity of indirect IF either of normal-human skin ($P=0.578$) or of 1 M NaCl-split skin ($P=0.709$) was not significantly different from ELISA of BP180 NC16a or C-terminal domain RPs (Table 1a, b). Most sera that are positive in indirect IF of normal-human skin or 1 M NaCl-split skin were also positive in BP180 NC16a domain RP ELISA ($P=0.578$), whereas normal-human skin they were not positive in IB of BP180 NC16a or C-terminal domain RPs ($P=0.057$). In addition, sensitivity of ELISA of the NC16a domain only ($P=0.022$), but not of NC16a and C-terminal domains ($P=0.176$) and of the C-terminal domain only ($P=0.344$), was significantly higher than that of the corresponding IB. These results showed that IF and ELISA, particularly IF, were generally more sensitive than IB.

Curiously, significant differences were found between the results of IB and ELISA using the same RP such as NC16a domain (Supplementary Table S1 online). We also noticed a similar difference in tests for BP sera (unpublished data). Different procedures for IB and ELISA may cause the discrepant results.

Finally, our studies of IB of epidermal extracts and ELISA of BP230 RPs detected anti-BP230 antibodies in only 10 patients, indicating that PNP sera may react with PNP-specific conformational epitopes on BP230, which are detected only by immunoprecipitation.

In this study, IF studies showed reactivity with BMZ in PNP patients. Combined results of IB of BP180 RPs and HaCaT, and of ELISAs of BP180 NC16a and C-terminal domain RPs showed that 42 and 40.67%, respectively, of PNP sera reacted with BP180. These results indicated that anti-BP180 autoantibodies are relatively frequently detected and have a role in BP-like blister formation in PNP.

CONFLICT OF INTEREST

The authors state no conflict of interest.

ACKNOWLEDGMENTS

We gratefully acknowledge Ms Michiru Kubo and Ms Kyoko Hiromatsu for technical assistance, and Ms Mihoko Ikeda, Ms Tomoko Tashima, Ms Shoko Nakamura, and Ms Mami Nishida for secretarial work. We thank the patients for their participation. This study was supported by Grants-in-Aid for Scientific Research (no. 20390308, 20591331, 21659271, 23591634, 23791298, 23791299, 23791300, 23791301, 24659534, 24591672, 24591640, 24791185), and Supported Program for the Strategic Research Foundation at Private Universities 2011–2015 from the Ministry of Education, Culture, Sports, Science and Technology; and by "Research on Measures for Intractable Diseases" Project: matching fund subsidy (H23-028 to K. Iwatsuki, and H24-038 to T. Hashimoto) from the Ministry of Health, Labour and Welfare. The study was also supported by grants from the Kaibara Morikazu Medical Science Promotion Foundation, Ishibashi Foundation, Kanae Foundation for the Promotion of Medical Science, Takeda Science Foundation, Chuo Mitsui Trust and Banking Company, Limited, and Nakatomi Foundation.

Author contributions

Tamihiro Kawakami contributed to this study mainly for statistical analyses as a part time instructor at Kurume University.

Atsunari Tsuchisaka[1], Hideo Kawano[1], Atsushi Yasukochi[1], Kwesi Teye[1], Norito Ishii[1], Hiroshi Koga[1], Ryosuke Sogame[1], Ayaka Ohzono[1], Rafal P. Krol[1], Tamihiro Kawakami[2], Minao Furumura[1], Chika Ohata[1], Xiaoguang Li[1] and Takashi Hashimoto[1]

[1]Department of Dermatology, Kurume University School of Medicine, and Kurume University Institute of Cutaneous Cell Biology, Kurume, Fukuoka, Japan and [2]Department of Dermatology, St Marianna University School of Medicine, Kawasaki, Kanagawa, Japan
E-mail: hashimot@med.kurume-u.ac.jp

SUPPLEMENTARY MATERIAL

Supplementary material is linked to the online version of the paper at http://www.nature.com/jid

REFERENCES

Anhalt GJ, Kim SC, Stanley JR *et al.* (1990) Paraneoplastic pemphigus. An autoimmune mucocutaneous disease associated with neoplasia. *N Engl J Med* 323:1729–35

Giudice GJ, Emery DJ, Diaz LA (1992) Cloning and primary structural analysis of the bullous pemphigoid autoantigen BP180. *J Invest Dermatol* 99:243–50

Hashimoto T (2001) Immunopathology of paraneoplastic pemphigus. *Clin Dermatol* 19:675–82

Hashimoto T, Ishii N, Ohata C *et al.* (2012) Pathogenesis of epidermolysis bullosa acquisita, an autoimmune subepidermal bullous disease. *J Pathol* 228:1–7

Ishii N, Ohyama B, Yamaguchi Z *et al.* (2008) IgA autoantibodies against the NC16a domain of BP180 but not 120-kDa LAD-1 detected in a patient with linear IgA disease. *Br J Dermatol* 158:1151–3

Matsumura K, Amagai M, Nishikawa T *et al.* (1996) The majority of bullous pemphigoid and herpes gestationis serum samples react with the NC16a domain of the 180-kDa bullous pemphigoid antigen. *Arch Dermatol Res* 288:507–9

Nie Z, Hashimoto T (1999) IgA antibodies of cicatricial pemphigoid sera specifically react with C-terminus of BP180. *J Invest Dermatol* 112:254–5

Oursler JR, Labib RS, Ariss-Abdo L *et al.* (1992) Human autoantibodies against desmoplakins in paraneoplastic pemphigus. *J Clin Invest* 89:1775–82

Preisz K, Horvath A, Sardy M *et al.* (2004) Exacerbation of paraneoplastic pemphigus by cyclophosphamide treatment: detection of novel autoantigens and bronchial autoantibodies. *Br J Dermatol* 150: 1018–24

Zillikens D, Caux F, Mascaro JM *et al.* (1999) Autoantibodies in lichen planus pemphigoides react with a novel epitope within the C-terminal NC16A domain of BP180. *J Invest Dermatol* 113:117–21

Type VII Collagen Is the Major Autoantigen for Sublamina Densa–Type Linear IgA Bullous Dermatosis

Journal of Investigative Dermatology (2015) **135,** 626–629; doi:10.1038/jid.2014.381; published online 23 October 2014

TO THE EDITOR

Linear IgA bullous dermatosis (LABD) is defined by IgA anti-basement membrane zone (BMZ) antibodies (Guide and Marinkovich, 2001). LABD is divided into two subgroups, lamina lucida–type and sublamina densa–type, which react with the epidermal and dermal sides of 1 M NaCl-split normal human skin, respectively, in indirect immunofluorescence (Willsteed *et al.*, 1990).

Most lamina lucida–type LABD sera react with the 97-kDa and 120-kDa LAD-1, truncated extracellular domains of BP180 (Zone *et al.*, 1990; Ishiko *et al.*, 1996; Ishii *et al.*, 2008). On the other hand, the autoantigen in sublamina densa–type LABD is still unclear, although a few cases reacted with type VII collagen (COL7) in previous immunoblotting studies (Rusenko *et al.*, 1989; Zambruno *et al.*, 1994; Hashimoto *et al.*, 1996).

In this study, we attempted to identify autoantigen for 12 sublamina densa–type LABD sera by immunofluorescence of COL7-lacked recessive dystrophic epidermolysis bullosa (RDEB) skin and ELISA of native trimer recombinant protein of full-length COL7 (Siprashvili *et al.*, 2010). Materials and Methods are described in Supplementary Materials online.

Twelve patient sera were sent to us from other institutes (11 and one patients from Japan and Spain, respectively) for our diagnostic studies. All patients showed typical clinical, histopathological, and immunopathological features.

The results of all immunological analyses for IgG and IgA antibodies in the 12 patients are summarized in Supplementary Table S1 online. Most patient sera showed negative IgG reactivity. Only one patient serum faintly reacted with epidermal side of 1 M NaCl-split skin. In IgA analyses, one serum showed reactivity with laminin γ2. We speculated that these reactivities were nonspecific, or these sera had autoantibodies to multiple antigens.

However, direct immunofluorescence performed in 11 patients showed only IgA deposition to BMZ, and indirect immunofluorescence of normal human skin detected only IgA anti-BMZ antibodies in 9 patient sera (Table 1). In addition, 10 sera reacted with dermal side of 1 M NaCl-split skin, whereas 2 sera reacted with both the epidermal and dermal sides (Table 1). These results strongly indicated that the 12 patients had sublamina densa–type LABD.

In IgA immunoblotting of normal human dermal extract, three of 12 patient sera and anti-COL7 mAb reacted with the 290-kDa COL7 (Figure 1a). Other patient sera and 16 normal control sera showed no reactivity.

In IgA post-embedding immune-electron microscopy of normal human skin section, unexpectedly, all sublamina densa–type LABD patient sera showed positive reactivity with the uppermost dermis at lamina lucida non-visible areas (Figure 1b, upper) but not at lamina densa visible areas (Figure 1b, lower). Epidermolysis bullosa acquisita serum reacted with lamina densa at both lamina lucida non-visible and visible areas (Figure 1e), as reported previously (Ishii *et al.*, 2004). We speculated that different fixation conditions during immune-electron microscopy procedure influenced the access of IgA

Table 1. Summaries of the results of all IgA immunofluorescence, immunoblotting, and ELISA studies

Patient no.	DIF	IIF of normal human skin	IIF of 1 M NaCl-split skin	IIF of RDEB skin	IB of dermal extract	ELISA of COL7 RP
1	BMZ+	BMZ+	E+, D+	BMZ−	−	*0.181*
2	BMZ+	BMZ+	D+	BMZ−	−	*0.229*
3	BMZ+	BMZ+	D+	BMZ−	−	*0.116*
4	ND	BMZ−	D+	BMZ−	−	0.045
5	BMZ+	BMZ+	D+	BMZ−	+	*0.198*
6	BMZ+	BMZ+	D+	BMZ−	−	0.057
7	BMZ+	BMZ−	E+, D±	BMZ−	+	*0.148*
8	BMZ+	BMZ+	D+	BMZ−	−	*0.142*
9	BMZ+	BMZ+	D+	BMZ−	−	0.079
10	BMZ+	BMZ+	D+	BMZ+	−	0.055
11	BMZ+	BMZ−	D+	BMZ−	+	*0.789*
12	BMZ+	BMZ+	D+	BMZ−	−	*0.214*

BMZ, basement membrane zone; COL7, type VII collagen; D, dermal side; DIF, direct immunofluorescence; E, epidermal side; IB, immunoblotting; IIF, indirect immunofluorescence; ND, not done; RDEB, recessive dystrophic epidermolysis bullosa; RP, recombinant protein; +, positive; ±, weakly positive; −, negative.
Numbers in italics denote positivity.

Abbreviations: BMZ, basement membrane zone; COL7, type VII collagen; LABD, linear IgA bullous dermatosis; RDEB, recessive dystrophic epidermolysis bullosa

Accepted article preview online 10 September 2014; published online 23 October 2014

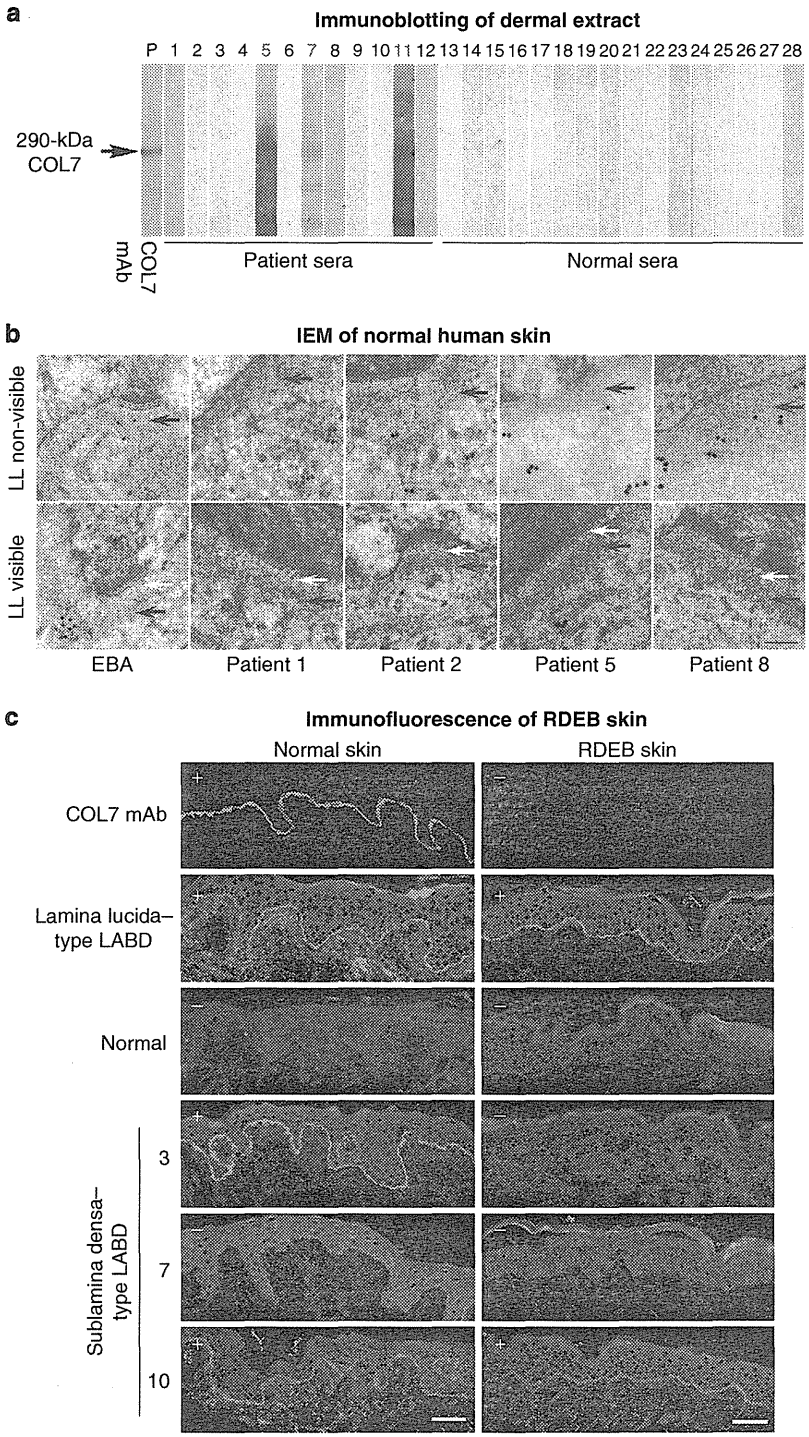

Figure 1. Immunological analyses of sublamina densa–type linear IgA bullous dermatosis (LABD). (**a**) Immunoblotting of normal human dermal extract for 12 patient (lanes 1–12) and 16 normal sera (lanes 13–28). Anti-COL7 monoclonal antibody (mAb) reacted with the 290-kDa COL7 (lane P). Red numbers: positive. (**b**) Post-embedding immune-electron microscopy (IEM) of normal human skin for Epidermolysis bullosa acquisita (EBA) serum (5 nm gold particles) and sera from sublamina densa–type LABD patients 1, 2, 5, and 8 (10 nm gold particles). Upper panel: lamina lucida (LL)–invisible. Lower panel: lamina lucida–visible. Black and white arrows indicate lamina densa and lamina lucida, respectively. Bar = 100 nm. (**c**) Indirect immunofluorescence of normal human and recessive dystrophic epidermolysis bullosa (RDEB) skin for anti-COL7 mAb, lamina lucida–type LABD serum, and sublamina densa–type LABD sera. +: positive reaction to basement membrane zone (BMZ), −: negative reaction to BMZ. Bars = 50 μm.

antibodies in the patient sera. Sera from patient 5, but not from patients 1, 2, and 8, reacted with COL7 by immunoblotting of the normal human dermal extract.

We next performed immunofluorescence using RDEB skin sections, similar to a previous study for epidermolysis bullosa acquisita (Liu *et al.*, 2003). The results of representative sera are depicted in Figure 1c, and the results of all sera tested are shown in Supplementary Figure S1 online. Anti-COL7 mAb showed no positive reactivity in RDEB skin, confirming complete lack of COL7 expression (Figure 1c). Anti-laminin γ1 pemphigoid patient sera, but not epidermolysis bullosa acquisita sera, reacted with BMZ in RDEB skin (data not shown). Eight of nine sublamina densa–type LABD sera positive in normal skin did not react with BMZ in RDEB skin, whereas a lamina lucida–type LABD serum reacted with BMZ. One sublamina densa–type LABD patient serum (patient 10) reacted with BMZ on RDEB skin (Figure 1c). None of the sublamina densa–type LABD sera negative in normal skin reacted with BMZ in RDEB skin either.

Although the results of immune-electron microscopy and immunofluorescence of RDEB skin suggested that most sublamina densa–type LABD patient sera reacted with COL7, only a few patient sera reacted with COL7 in immunoblotting of normal human dermal extract. We considered that this discrepancy was due to the loss of conformation of COL7 during the immunoblotting procedure.

We then performed IgA ELISA using the commercially available ELISA kit, which used mammalian recombinant protein with combined NC1 and NC2 domains of COL7 (Medical and Biological Laboratories, Nagoya, Japan). However, in this ELISA, only one patient serum showed positive reactivity (data not shown).

Therefore, we developed IgA ELISA. Trimer form recombinant protein of full-length mammalian COL7 (Siprashvili *et al.*, 2010) and Can Get Signal Immunoreaction Enhancer Solution (Toyobo, Tokyo, Japan) were used for detecting autoantibodies to COL7 in patient sera. The bound autoantibodies were detected by the HRP detection system using anti-human IgA-HRP (Medical and Biological Laboratories, Nagoya, Japan) and TMB (Moss, Pasadena, MD). Technical details are described in Supplementary Materials online.

In this ELISA, eight sublamina densa–type LABD patient sera showed positive results, whereas all 16 normal control sera were negative (Table 1). Lamina lucida type–LABD, bullous pemphigoid, pemphigus vulgaris, and pemphigus foliaceus sera did not show positive reaction in the IgA ELISA analyses (Supplementary Figure S2 online). The results of this ELISA for three representative sera at different dilutions indicated that the results were in a linear range (Supplementary Figure S3 online). The different results between commercial ELISA and developed ELISA in this study may indicate that IgA autoantibodies in patient sera reacted with conformational epitopes in the collagenous domain of COL7 but not NC1 and NC2 domains.

The results of all studies in this study are summarized in Table 1. As previous immunoblotting studies, only 3 of 12 sublamina densa–type LABD patient sera reacted with COL7 by conventional immunoblotting of normal human dermal extract. In contrast, most patient sera were confirmed to react with COL7 by the results obtained in indirect immunofluorescence of RDEB skin and ELISA of COL7 trimer recombinant protein. The results between immunofluorescence and ELISA studies were almost consistent.

In this study, in addition to three patients positive with COL7 in conventional immunoblotting, two additional analyses confirmed the reactivity with COL7 in five patients, although autoantigens in four patients were still unknown. The results in this study indicated that COL7 is the major autoantigen in sublamina densa–type LABD.

All studies were conducted under the approval of the Ethics Committee of Kurume University School of Medicine and according to the Declaration of Helsinki Principles. Written informed consent was obtained from all patients and normal control individuals.

CONFLICT OF INTEREST

The authors state no conflict of interest.

ACKNOWLEDGMENTS

We gratefully acknowledge Ms Michiru Kubo and Ms Kyoko Hiromatsu for the technical assistance, and Ms Mihoko Ikeda, Ms Tomoko Tashima, and Ms Mami Nishida for the secretarial work. We thank the patients for their participation. This study was supported by Grants-in-Aid for Scientific Research (nos. 20390308, 20591331, 21659271, 23591634, 23791298, 23791299, 23791300, 23791301, 24659534, 24591672, 24591640, 24791185), by the Supported Program for the Strategic Research Foundation at Private Universities from the Ministry of Education, Culture, Sports, Science and Technology, and by the "Research on Measures for Intractable Diseases" Project: matching fund subsidy (H23-028 to K. Iwatsuki, and H24-038 to T. Hashimoto) from the Ministry of Health, Labour, and Welfare. The study was also supported by grants from the Kaibara Morikazu Medical Science Promotion Foundation, Ishibashi Foundation, Kanae Foundation for the Promotion of Medical Science, Takeda Science Foundation, Chuo Mitsui Trust and Banking Company, Limited, and Nakatomi Foundation.

Atsunari Tsuchisaka[1], Koji Ohara[1], Norito Ishii[1], Ngon T. Nguyen[2], M. Peter Marinkovich[2,3] and Takashi Hashimoto[1]

[1]Department of Dermatology, Kurume University School of Medicine, and Kurume University Institute of Cutaneous Cell Biology, Fukuoka, Japan; [2]Department of Dermatology, Stanford University School of Medicine, Center for Clinical Sciences Research, Stanford, California, USA and [3]Division of Dermatology, Palo Alto Veterans Affairs Medical Center, Palo Alto, California, USA.
E-mail: hashimot@med.kurume-u.ac.jp

SUPPLEMENTARY MATERIAL

Supplementary material is linked to the online version of the paper at http://www.nature.com/jid

REFERENCES

Guide SV, Marinkovich MP (2001) Liner IgA bullous dermatosis. *Clin Dermatol* 19:719–27

Hashimoto T, Ishiko A, Shimizu H *et al.* (1996) A case of linear IgA bullous dermatosis with IgA anti-type VII collagen autoantibodies. *Br J Dermatol* 134:336–9

Ishiko A, Shimizu H, Masunaga T *et al.* (1996) 97-kDa linear IgA bullous dermatosis (LAD) antigen lozalizes to the lamina lucida of the epidermal basement membrane. *J Invest Dermatol* 106:739–43

Ishii N, Yoshida M, Hisamatsu Y *et al.* (2004) Epidermolysis bullosa acquisita sera react with distinct epitopes on the NC1 and NC2 domains of type VII collagen: study using immunoblotting of domain-specific recombinant proteins and postembedding immunoelectron microscopy. *Br J Dermatol* 150:843–51

Ishii N, Ohyama B, Yamaguchi Z *et al.* (2008) IgA autoantibodies against the NC16a domain of

BP180 but not 120-kDa LAD-1 detected in a patient with linear IgA disease. *Br J Dermatol* 158:1151–3

Liu Y, Shimizu H, Hashimoto T (2003) Immunofluorescence studies using skin sections of recessive dystrophic epidermolysis bullosa patients indicates that the antigen of anti-p200 pemphigoid is not a fragment of type VII collagen. *J Dermatol Sci* 32:125–9

Rusenko KW, Gammon WR, Briggaman RA (1989) Type VII collagen is the antigen recognized by IgA anti-sub lamina densa autoantibodies. *J Invest Dermatol* 92:510, (Abstr.)

Siprashvili Z, Nguyen NT, Bezchinsky MY *et al.* (2010) Long-term type VII collagen restriction to human epidermolysis bullosa skin tissue. *Hum Gene Ther* 21:1299–310

Willsteed E, Bhogal BS, Black MM *et al.* (1990) Use of 1M NaCl split skin in the direct immunofluorescence of the liner IgA bullous dermatoses. *J Cutan Pathol* 17:144–8

Zambruno G, Manca V, Kanitakis J *et al.* (1994) Linear IgA bullous dermatosis with autoantibodies to a 290 kd antigen of anchoring fibrils. *J Am Acad Dermatol* 31: 884–8

Zone JJ, Taylor TB, Kadunce DP *et al.* (1990) Identification of the cutaneous basement membrane zone antigen and isolation of antibody in linear immunoglobulin - A bullous dermatosis. *J Clin Invest* 85: 812–20

nature immunology

Perivascular leukocyte clusters are essential for efficient activation of effector T cells in the skin

Yohei Natsuaki[1,2,15], Gyohei Egawa[1,15], Satoshi Nakamizo[1], Sachiko Ono[1], Sho Hanakawa[1], Takaharu Okada[3], Nobuhiro Kusuba[1], Atsushi Otsuka[1], Akihiko Kitoh[1], Tetsuya Honda[1], Saeko Nakajima[1], Soken Tsuchiya[4], Yukihiko Sugimoto[4], Ken J Ishii[5,6], Hiroko Tsutsui[7], Hideo Yagita[8], Yoichiro Iwakura[9,10], Masato Kubo[11,12], Lai guan Ng[13], Takashi Hashimoto[2], Judilyn Fuentes[14], Emma Guttman-Yassky[14], Yoshiki Miyachi[1] & Kenji Kabashima[1]

It remains largely unclear how antigen-presenting cells (APCs) encounter effector or memory T cells efficiently in the periphery. Here we used a mouse contact hypersensitivity (CHS) model to show that upon epicutaneous antigen challenge, dendritic cells (DCs) formed clusters with effector T cells in dermal perivascular areas to promote *in situ* proliferation and activation of skin T cells in a manner dependent on antigen and the integrin LFA-1. We found that DCs accumulated in perivascular areas and that DC clustering was abrogated by depletion of macrophages. Treatment with interleukin 1α (IL-1α) induced production of the chemokine CXCL2 by dermal macrophages, and DC clustering was suppressed by blockade of either the receptor for IL-1 (IL-1R) or the receptor for CXCL2 (CXCR2). Our findings suggest that the dermal leukocyte cluster is an essential structure for elicitating acquired cutaneous immunity.

Boundary tissues, including the skin, are continually exposed to foreign antigens, which must be monitored and possibly eliminated. Upon exposure to foreign antigens, skin dendritic cells (DCs), including epidermal Langerhans cells (LCs), capture the antigens and migrate to draining lymph nodes (LNs), where the presentation of antigen to naive T cells occurs mainly in the T cell zone. In this location, the accumulation of naive T cells in the vicinity of DCs is mediated by signaling via the chemokine receptor CCR7 (ref. 1). The T cell zone in the draining LNs facilitates the efficient encounter of antigen-bearing DCs with antigen-specific naive T cells.

In contrast to T cells in LNs, the majority of T cells in the skin, including infiltrating skin T cells and skin-resident T cells, have an effector-memory phenotype[2]. In addition, the presentation of antigen to skin T cells by antigen-presenting cells (APCs) is the crucial step in the elicitation of acquired skin immune responses, such as contact dermatitis. Therefore, we investigated how antigen presentation occurs in the skin and if it is different from antigen presentation in LNs. Published studies using mouse contact hypersensitivity (CHS) as a model of human contact dermatitis have revealed that dermal DCs (dDCs) have a pivotal role in the transport and presentation of antigen to the LNs, but epidermal LCs do not[3]. In the skin, however, it remains unclear which subset of APCs presents antigens to skin T cells and how skin T cells efficiently encounter APCs. In addition, dermal macrophages are key modulators in CHS responses[4], but the precise mechanisms by which macrophages are involved in the recognition of antigen in the skin have not yet been clarified. These unanswered questions prompted us to investigate where skin T cells recognize antigens and how skin T cells are activated in the elicitation phase of acquired cutaneous immune responses such as CHS.

When keratinocytes encounter foreign antigens, they immediately produce various proinflammatory mediators, such as interleukin 1 (IL-1) and tumor-necrosis factor, in an antigen-nonspecific manner[5,6]. Proteins of the IL-1 family are considered important modulators in CHS responses because the activation of hapten-specific T cells is impaired in mice deficient in both IL-1α and IL-1β but not in mice deficient in tumor-necrosis factor[7]. IL-1α and IL-1β are agonistic ligands of the receptor for IL-1 (IL-1R). While IL-1α is stored in keratinocytes and is secreted upon exposure to nonspecific stimuli, IL-1β is produced mainly by epidermal LCs and dermal mast cells in an inflammasome-dependent manner via activation of the cytoplasmic pattern-recognition receptor NLRP3 and of caspase-1 and caspase-11. Because IL-1α and IL-1β are crucial in the initiation of acquired

[1]Department of Dermatology, Kyoto University Graduate School of Medicine, Kyoto, Japan. [2]Department of Dermatology, Kurume University School of Medicine, Fukuoka, Japan. [3]Research Unit for Immunodynamics, RIKEN Research Center for Allergy and Immunology, Kanagawa, Japan. [4]Department of Pharmaceutical Biochemistry, Graduate School of Pharmaceutical Sciences, Kumamoto University, Kumamoto, Japan. [5]Laboratory of Adjuvant Innovation, National Institute of Biomedical Innovation, Osaka, Japan. [6]Laboratory of Vaccine Science, WPI Immunology Frontier Research Center, Osaka University, Osaka, Japan. [7]Department of Microbiology, Hyogo College of Medicine, Hyogo, Japan. [8]Department of Immunology, Juntendo University School of Medicine, Tokyo, Japan. [9]Research Institute for Biomedical Sciences, Tokyo University of Science, Chiba, Japan. [10]Medical Mycology Research Center, Chiba University, Chiba, Japan. [11]Laboratory for Cytokine Regulation, RIKEN center for Integrative Medical Science, Kanagawa, Japan. [12]Division of Molecular Pathology, Research Institute for Biomedical Science, Tokyo University of Science, Chiba, Japan. [13]Singapore Immunology Network, Agency for Science, Technology and Research, Biopolis, Singapore. [14]Department of Dermatology, Icahn School of Medicine at Mount Sinai School Medical Center, New York, New York, USA. [15]These authors contributed equally to this work. Correspondence should be addressed to K.K. (kaba@kuhp.kyoto-u.ac.jp).

Received 7 July; accepted 19 August; published online 21 September 2014; doi:10.1038/ni.2992

immune responses such as CHS, it is of great interest to understand how IL-1 modulates the recognition of antigen by skin T cells.

Using a mouse CHS model, here we examined how DCs and effector T cells encounter each other efficiently in the skin. We found that upon encountering antigenic stimuli, dDCs formed clusters in which effector T cells were activated and proliferated in an antigen-dependent manner. These DC–T cell clusters were initiated by skin macrophages via IL-1R signaling and were essential for the establishment of cutaneous acquired immune responses.

RESULTS

Formation of DC–T cell clusters at antigen-challenged sites

To explore the accumulation of cells of the immune system in the skin, we examined the clinical and histological features of the elicitation of human allergic contact dermatitis. Allergic contact dermatitis is the most common of eczematous skin diseases, affecting 15–20% of the general population worldwide[8], and is mediated by T cells. Although antigens should be spread evenly over the surface of skin, clinical manifestations commonly include discretely distributed small vesicles (**Fig. 1a**), which suggests an uneven occurrence of intense inflammation. Histological examination of allergic contact dermatitis showed spongiosis, intercellular edema in the epidermis and colocalization of perivascular infiltrates of $CD3^+$ T cells and spotty accumulation of $CD11c^+$ DCs in the dermis, especially beneath the vesicles (**Fig. 1b**). These findings led us to hypothesize that focal accumulation of T cells and DCs in the dermis might contribute to vesicle formation in early eczema.

To characterize the DC–T cell clusters in elicitation reactions, we used two-photon microscopy to obtain time-lapse images in a mouse model of CHS. We isolated T cells from the draining LNs of mice sensitized with the hapten DNFB (2,4-dinitrofluorobenzene), labeled the cells with fluorescent dye and transferred them into mice that express the common DC marker CD11c tagged with yellow fluorescent protein (YFP). In the steady state, YFP^+ dDCs distributed diffusely (**Fig. 1c**), representative of nondirected movement in a random fashion (**Supplementary Fig. 1**), as reported before[9]. After topical challenge with DNFB, YFP^+ dDCs transiently increased their velocity and formed clusters in the dermis, with the clusters becoming larger and more evident after 24 h (**Fig. 1c** and **Supplementary Movie 1**). At the same time, transferred T cells accumulated in the DC clusters and interacted with YFP^+ DCs for several hours (**Fig. 1d** and **Supplementary Movie 2**). Thus, we observed accumulation of DCs and T cells in the dermis in mice during CHS responses. We noted that the intercellular spaces between keratinocytes overlying the DC–T cell clusters in the dermis were enlarged (**Fig. 1e**), which replicated observations made for human allergic contact dermatitis (**Fig. 1b**).

We next sought to determine which of the two main DC populations in skin, epidermal LCs or dDCs, was essential for the elicitation of CHS. To deplete mice of all cutaneous DC subsets, we used mice with sequence expressing the diphtheria toxin receptor (DTR) under the control of the promoter of the gene encoding langerin as recipients (in such 'Langerin-DTR' mice, treatment with diphtheria toxin (DT) leads to depletion of langerin-positive cells) and mice that express a transgene encoding DTR under the control of promoter of the gene encoding CD11c as donors (in such 'CD11c-DTR' mice, treatment with DT leads to transient depletion of $CD11c^+$ DC populations). To selectively deplete mice of LCs or dDCs, we transferred bone marrow (BM) cells from C57BL/6 mice or CD11c-DTR mice into Langerin-DTR or C57BL/6 mice, respectively (**Supplementary Fig. 2a,b**). We injected DT into the chimeras to ensure depletion of each DC subset before elicitation and found that ear swelling and inflammatory histological findings were significantly attenuated in the absence of dDCs but not in the absence of LCs (**Fig. 1f** and **Supplementary Fig. 2c**). In addition, production of interferon-γ (IFN-γ) in skin T cells was substantially suppressed in mice depleted of dDCs (**Fig. 1g**). These results suggested that dDCs, not epidermal LCs, were essential for T cell activation and the elicitation of CHS responses.

Antigen-dependent proliferation of skin effector T cells *in situ*

To evaluate the effect of DC–T cell clusters in the dermis, we determined whether T cells had acquired the ability to proliferate via the accumulation of DC–T cell clusters in the dermis. We purified $CD4^+$ or $CD8^+$ T cells from the draining LNs of DNFB-sensitized mice, labeled

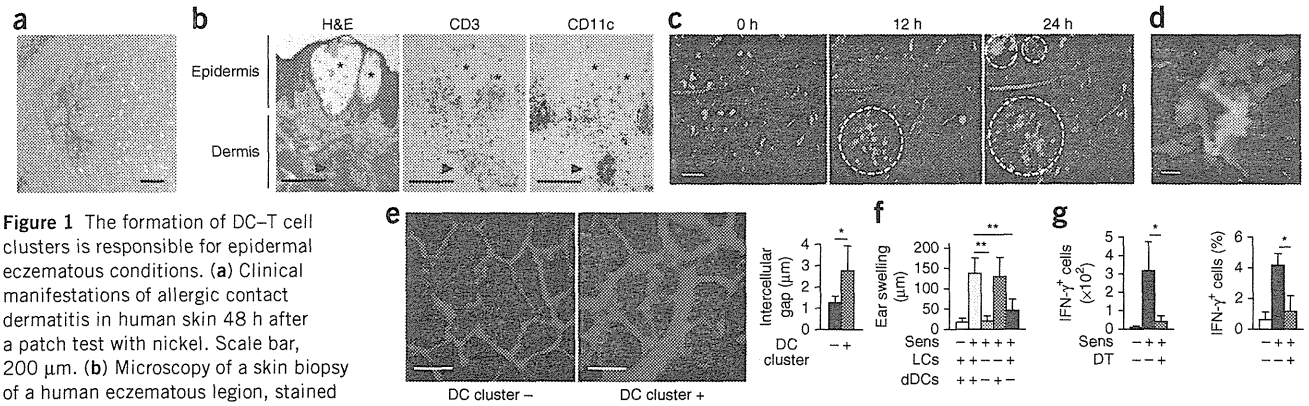

Figure 1 The formation of DC–T cell clusters is responsible for epidermal eczematous conditions. (**a**) Clinical manifestations of allergic contact dermatitis in human skin 48 h after a patch test with nickel. Scale bar, 200 μm. (**b**) Microscopy of a skin biopsy of a human eczematous legion, stained with hematoxylin and eosin (H&E) or with antibody to CD3 (anti-CD3) or anti-CD11c. *, epidermal vesicles; arrowheads indicate dDC–T cell clusters. Scale bars, 250 μm. (**c**) Sequential images of leukocyte clusters in the elicitation phase of CHS. White outlined areas indicate dermal accumulation of DCs (green) and T cells (red). Scale bar, 100 μm. (**d**) Enlargement of DC–T cell cluster in **c**. Scale bar,10 μm. (**e**) Intercellular edema of the epidermis overlying a DC–T cell cluster in the dermis, with keratinocytes (red) visualized with isolectin B4 (left), and distance between adjacent keratinocytes above (+) or not above (–) a DC–T cell cluster ($n = 20$ images per condition) (right). Scale bars, 10 μm. (**f**) Ear swelling 24 h after CHS with (+) or without (–) sensitization (Sens) and with (–) or without (+) subset-specific depletion of DCs ($n = 5$ mice per group). (**g**) Quantification (left) and frequency (right) of IFN-γ-producing T cells in the ear 18 h after CHS with or without sensitization (as in **f**) and with (DT +) or without (DT –) depletion of dDCs ($n = 5$ mice per group). $^*P < 0.05$ and $^{**}P < 0.001$ (unpaired Student's *t*-test). Data are representative of five independent experiments (**a–d**) or three experiments (**f,g**) or are pooled from three experiments (**e**; error bars (**e–g**), s.d.).

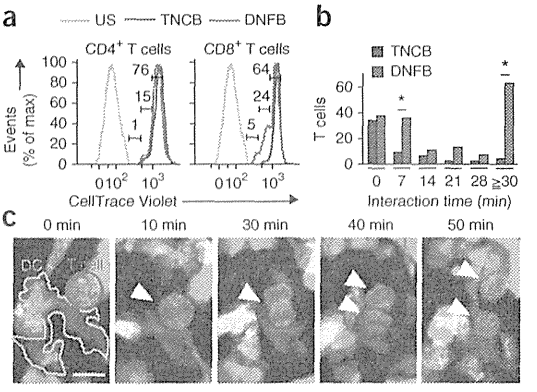

Figure 2 Antigen-dependent T cell proliferation in DC–T cell clusters. (**a**) Proliferation $CD4^+$ T cells (left) or $CD8^+$ T cells (right) in the skin of recipient mice 24 h after transfer of CellTrace Violet–labeled cells from donor mice left unsensitized (US) or sensitized with DNFB or TNCB, assessed as dilution of tracer in the challenged sites. Numbers adjacent to bracketed lines indicate percent cells that had proliferated. (**b**) Conjugation time of dDCs with T cells sensitized with DNFB ($n = 160$ T cells) or TNCB ($n = 60$ T cells), assessed at 24 h after challenge with DNFB. $^*P < 0.05$ (unpaired Student's *t*-test). (**c**) Sequential images of dividing T cells (red) in DC–T cell clusters. Green, dDCs; arrowheads indicate a dividing T cell. Data are representative of three experiments.

the cells with a division-tracking dye and transferred the cells into naive mice. Twenty-four hours after the application of DNFB to the recipient mice, we collected the skin to evaluate T cell proliferation by dilution of fluorescence intensity. Most of the infiltrating T cells (>90%) were $CD44^+CD62L^-$ effector T cells (**Supplementary Fig. 2d**). Among the infiltrating T cells, $CD8^+$ T cells proliferated actively, whereas the $CD4^+$ T cells showed low proliferative potency (**Fig. 2a**). This T cell proliferation was antigen dependent because T cells sensitized with the hapten TNCB (2,4,6-trinitrochlorobenzene) exhibited low proliferative activity in response to the application of DNFB (**Fig. 2a**). In line with that finding, the DC–T cell conjugation time was prolonged in the presence of the cognate antigen DNFB (**Fig. 2b**), and the T cells interacting with DCs within DC–T cell clusters proliferated (**Fig. 2c** and **Supplementary Movie 3**). These findings indicated that skin effector T cells conjugated with DCs and proliferated *in situ* in an antigen-dependent manner.

LFA-1-dependent activation of $CD8^+$ T cells in DC–T cell clusters

Sustained interaction between DCs and naive T cells, known as the 'immunological synapse', is maintained by cell adhesion molecules[10]. In particular, the integrin LFA-1 (CD58) on T cells binds to cell-surface glycoproteins, such as the intercellular adhesion molecule ICAM-1, on APCs, which is essential for the proliferation and activation of naive T cells during antigen recognition in the LNs. To determine whether LFA-1–ICAM-1 interactions are required for the activation of effector T cells in DC–T cell clusters in the skin, we elicited a CHS response in mouse ear skin with DNFB, then injected KBA, a neutralizing antibody to LFA-1, intravenously 14 h later. Such administration of KBA reduced the accumulation of T cells in the dermis (**Fig. 3a**). The velocity of T cells in the cluster was 0.65 ± 0.29 μm/min (mean ± s.d.) at 14 h after the DNFB challenge and increased up to threefold (1.64 ± 1.54 μm/min) at 8 h after treatment with KBA, while it was not affected by treatment with the isotype-matched control antibody immunoglobulin G (IgG) (**Fig. 3b**). At the outside of clusters, T cells smoothly migrated at the mean velocity of 2.95 ± 1.19 μm/min, consistent with published results[11], and this was not affected by treatment with the control antibody IgG (data not shown). Treatment with KBA also significantly attenuated ear swelling (**Fig. 3c**) as well as IFN-γ production by skin $CD8^+$ T cells (**Fig. 3d,e**). These results suggested that the DC–effector T cell conjugates were integrin dependent, similar to the DC–naive T cell interactions in draining LNs.

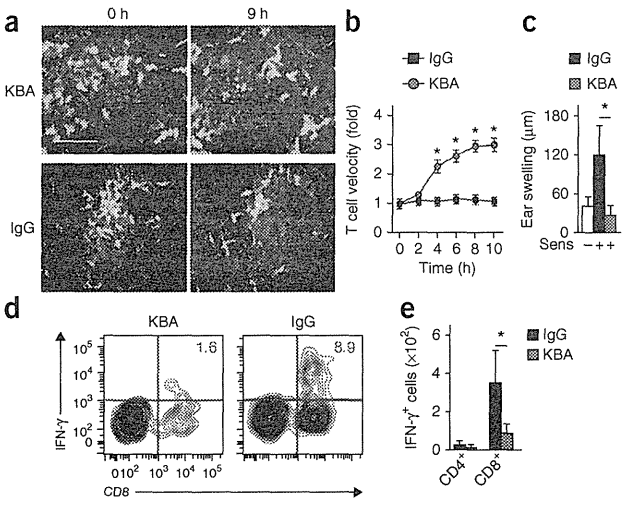

dDC clustering requires skin macrophages

We next examined the factors that initiated the accumulation of DC–T cell clusters. dDC clusters also formed in response to the initial application of hapten (sensitization phase), but their number decreased significantly 48 h after sensitization, while DC clusters persisted for 48 h in the elicitation phase (**Fig. 4a** and **Supplementary Fig. 3a**). These DC clusters were abrogated 7 d after application of DNFB (data not shown). These observations suggested that the accumulation of DC–T cell clusters was initiated by DC clustering, which then induced the accumulation, proliferation and activation of T cells, a process that depended on the presence of antigen-specific effector T cells *in situ*. DC clusters were also induced by solvents (such as acetone) or adjuvants (such as dibutylphthalic acid) and by pathogenic inoculation with *Mycobacterium bovis* bacillus Calmette-Guérin (**Supplementary Fig. 3b,c**). In addition, we observed DC clusters not only in the ear skin but also in other regions, such as the back skin and the footpad (**Supplementary Fig. 3d**). These results suggested that the formation of DC clusters was not an ear-specific event but was a general mechanism during skin inflammation.

The abundance of DC clusters in response to the application of DNFB was not altered in mice that lack T cells and B cells (recombinase

Figure 3 LFA-1 is essential for the persistence of DC–T cell clustering and for T cell activation in the skin. (**a**) Clusters of DCs (green) and T cells (red) in the DNFB-challenged site before (0 h) and 9 h after treatment with KBA (LFA-1-neutralizing antibody) or IgG (isotype-matched control antibody). Scale bar, 100 μm. (**b**) T cell velocity in DNFB-challenged sites at various times (horizontal axis) after treatment with KBA or IgG ($n = 30$ T cells per group), presented relative to velocity at time 0, set as 1. (**c**) Ear swelling 24 h after treatment with KBA or IgG in mice ($n = 5$ per group) left unsensitized (Sens –) or challenged with DNFB (Sens +). (**d,e**) IFN-γ production by $CD8^+$ T cells (**d**) and quantification of IFN-γ-producing cells in the $CD4^+$ or $CD8^+$ population (**e**) in skin from mice ($n = 5$ per group) challenged with DNFB, then treated with KBA or IgG 12 h later, assessed 6 h after antibody treatment. Numbers in top right quadrants (**d**) indicate percent $IFN\text{-}\gamma^+CD8^+$ T cells. $^*P < 0.05$ (unpaired Student's *t*-test). Data are representative of three experiments (error bars (**b,c,e**), s.d.).

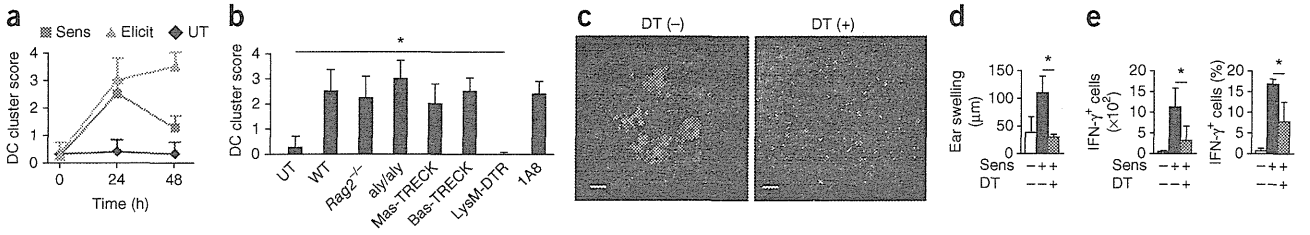

Figure 4 Macrophages are essential for DC cluster formation. (**a**) Score of DC cluster abundance in mice ($n = 4$ per group) left untreated (UT) or 24 h and 48 h after application of DNFB in the sensitization or elicitation phase of CHS; scores were assigned according to the size and number of clusters. (**b**) Score of DC cluster abundance (as in **a**) in untreated wild-type mice (UT), in DNFB-treated wild-type (C57BL/6) mice (WT), RAG-2-deficient mice (*Rag2*$^{-/-}$), aly/aly mice (aly/aly), DT-treated Mas-TRECK or Bas-TRECK mice or DT-treated C57BL/6 recipients of LysM-DTR BM cells, and in wild-type mice treated with 1A8 (anti-Ly6G) ($n = 4$ mice per group). (**c**) DC clusters in C57BL/6 chimeras given LysM-DTR BM with (right) or without (left) treatment of recipients with DT. Scale bars, 100 μm. (**d**) Ear swelling in C57BL/6 chimeras ($n = 5$ per group) given LysM-DTR BM with or without treatment with DT, assessed 24 h after no DNFB (Sense −) or application of DNFB to the recipients. (**e**) Quantification (left) and frequency (right) of IFN-γ-producing CD8$^+$ T cells in mice as in **d** ($n = 5$ per group). *$P < 0.05$ (unpaired Student's *t*-test). Data are representative of three (**a**,**c**,**e**), two (**b**) or four (**d**) experiments (error bars (**b**,**d**,**e**), s.d.).

RAG-2–deficient mice), in mice deficient in lymphoid tissue–inducer cells (alymphoblastic (aly/aly) mice)[12] or in mice depleted of mast cells or basophils (Mas-TRECK or Bas-TRECK mice treated with DT)[13,14] (**Fig. 4b**). In contrast, DC clustering was abrogated in C57BL/6 mice given transfer of BM from LysM-DTR mice (with sequence encoding a DTR cassette inserted into the gene encoding lysozyme M) followed by treatment of the recipients with DT to ensure depletion of both macrophages and neutrophils (**Fig. 4b**,**c**). Depletion of neutrophils alone, by administration of antibody 1A8 to Ly6G, did not interfere with the formation of DC clusters (**Fig. 4b**), which suggested that macrophages were required during the formation of DC clusters, but neutrophils were not. Of note, the formation of DC clusters was not attenuated by treatment with the LFA-1-neutralizing antibody KBA (**Supplementary Fig. 3e**,**f**), which suggested that macrophage-DC interactions were LFA-1 independent. Consistent with the formation of DC clusters, elicitation of the CHS response (**Fig. 4d**) and IFN-γ production by skin T cells (**Fig. 4e**) were significantly suppressed in chimeras given LysM-DTR BM and treated with DT. Thus, skin macrophages were required for the formation of DC clusters, which was necessary for T cell activation and the elicitation of CHS.

Perivascular DCs clustering requires macrophages

To examine the migratory kinetics of dermal macrophages and DCs *in vivo*, we visualized them by two-photon microscopy. *In vivo* labeling of blood vessels with dextran conjugated to the hydrophobic red fluorescent dye TRITC (tetramethylrhodamine isothiocyanate) revealed that dDCs distributed diffusely in the steady state (**Fig. 5a**, left). After application of DNFB to the ears of mice previously sensitized with DNFB, dDCs accumulated mainly around post-capillary venules (**Fig. 5a**, right, and **b**). Time-lapse imaging revealed that some dDCs showed directional migration toward TRITC$^+$ cells that were labeled red by incorporation of extravasated TRITC-dextran (**Fig. 5c** and **Supplementary Movie 4**). Most of the TRITC$^+$ cells were F4/80$^+$CD11b$^+$ macrophages (**Supplementary Fig. 4a**). These observations prompted us to investigate the role of macrophages in DC accumulation. We used a chemotaxis assay to determine whether macrophages attracted the DCs. We isolated dDCs and dermal macrophages from dermal skin cell suspensions and incubated them for 12 h in a Transwell assay. dDCs placed in the upper wells migrated efficiently to lower wells that contained dermal macrophages (**Fig. 5d**). However, we did not observe such dDC migration when macrophages were absent from the lower wells (**Fig. 5d**). Thus, dermal macrophages were able to attract dDCs *in vitro*, which may have led to the accumulation of dDCs around post-capillary venules.

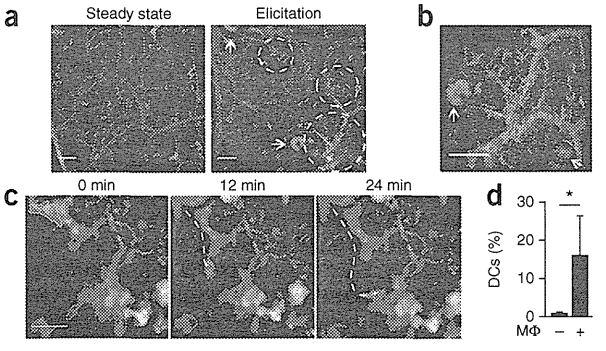

Figure 5 Macrophages mediate the perivascular formation of DC clusters. (**a**) Distribution of dDCs (green) in the steady state (left) and in the elicitation phase of CHS (right). White outlined areas indicate DC clusters; arrows indicate sebaceous glands visualized with BODIPY (green); yellow and red, blood vessels; red, macrophages. Scale bars, 100 μm. (**b**) Enlargement of a perivascular DC cluster. Arrows indicate sebaceous glands of hair follicles. Scale bar, 100 μm.(**c**) Sequential images of dDCs (green) and macrophages (red) in the elicitation phase of CHS. White dashed line represents the track of a DC. Scale bar, 30 μm. (**d**) Chemotaxis of dDCs in the presence (+) or absence (−) of macrophages (MΦ) prepared from ear skin, presented as the frequency of dDCs that transmigrated into the lower chamber of a Transwell (relative to input dDCs). *$P < 0.05$ (unpaired Student's *t*-test). Data are representative of three experiments (error bars (**d**), s.d.).

DC cluster formation requires IL-1α upon antigen challenge

We attempted to explore the mechanism underlying the formation of DC clusters. We observed that DC accumulation occurred during the first application of hapten (**Fig. 4a**), which suggested that an antigen-nonspecific mechanism, such as production of the proinflammatory mediator IL-1, may initiate DC clustering. DNFB-induced accumulation of DCs was not suppressed in mice deficient in NLRP3 or deficient in caspase-1 and caspase-11 more than their wild-type counterparts, but it was significantly lower in IL-1R1-deficient mice (which lack the receptor for IL-1α and IL-1β and for the IL-1 receptor antagonist (IL-1ra)) than in their wild-type counterparts, as well as after the subcutaneous administration of IL-1ra than before treatment with the antagonist (**Fig. 6a**,**b**). Consistent with those observations, the elicitation of CHS and IFN-γ production by skin T cells were significantly attenuated in mice that lacked both IL-1α and IL-1β (**Fig. 6c**,**d**). In addition, the formation of dDC clusters was suppressed significantly by the subcutaneous injection of a neutralizing antibody to IL-1α but

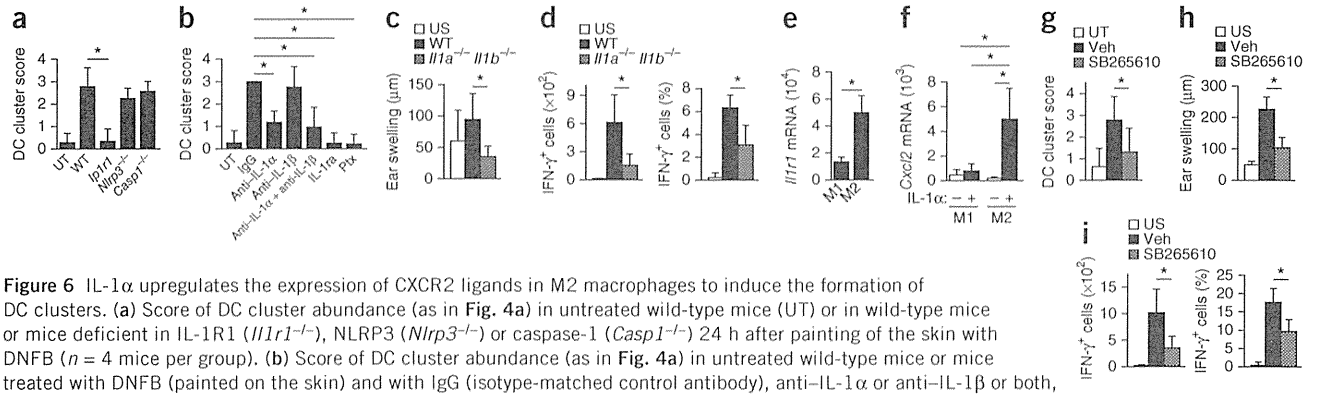

Figure 6 IL-1α upregulates the expression of CXCR2 ligands in M2 macrophages to induce the formation of DC clusters. (**a**) Score of DC cluster abundance (as in **Fig. 4a**) in untreated wild-type mice (UT) or in wild-type mice or mice deficient in IL-1R1 (*Il1r1*$^{-/-}$), NLRP3 (*Nlrp3*$^{-/-}$) or caspase-1 (*Casp1*$^{-/-}$) 24 h after painting of the skin with DNFB ($n = 4$ mice per group). (**b**) Score of DC cluster abundance (as in **Fig. 4a**) in untreated wild-type mice or mice treated with DNFB (painted on the skin) and with IgG (isotype-matched control antibody), anti–IL-1α or anti–IL-1β or both, recombinant IL-1ra or pertussis toxin (Ptx), assessed 24 h after treatment with hapten ($n = 4$ mice per group). (**c**,**d**) Ear swelling 24 h after application of DNFB (**c**) and quantification (**d**, left) and frequency (**d**, right) of IFN-γ-producing CD8$^+$ T cells in the ear 18 h after application of DNFB (**d**) in unsensitized wild-type mice (US) or in mice lacking both IL-1α and IL-1β (*Il1a*$^{-/-}$*Il1b*$^{-/-}$) and wild-type mice given adoptive transfer of DNFB-sensitized T cells ($n = 5$ mice per group). (**e**) Quantitative RT-PCR analysis of *Il1r1* mRNA in M1 or M2 macrophages ($n = 4$ mice per group). (**f**) Quantitative RT-PCR analysis of *Cxcl2* mRNA in M1 or M2 macrophages cultured with (+) or without (−) IL-1α. (**g**) Score of DC cluster abundance (as in **Fig. 4a**) in untreated wild-type mice (UT) or in mice treated with DNFB (painted on the skin) in the presence (SB265610) or absence (vehicle (Veh)) of a CXCR2 inhibitor, assessed 24 h after treatment with DNFB ($n = 4$ mice per group). (**h**,**i**) Ear swelling 24 h after application of DNFB (**h**) and quantification (**i**, right) and frequency (**i**, left) of IFN-γ-producing CD8$^+$ T cells 18 h after application of DNFB (**i**) in unsensitized wild-type mice (US) or in mice treated with DNFB in the presence or absence of the CXCR2 inhibitor SB265610 ($n = 5$ mice per group). *$P < 0.05$ (unpaired Student's *t*-test). Data are representative of two (**a**,**c**,**d**) or three (**b**,**e**–**i**) experiments (error bars, s.d.).

was suppressed only marginally by a neutralizing antibody to IL-1β (**Fig. 6b**). Because keratinocytes are known to produce IL-1α upon application of a hapten[15], our results suggested a major role for IL-1α in mediating the formation of DC clustering.

M2 macrophages produce chemokine CXCL2 to attract dDCs

To further characterize how macrophages attract dDCs, we examined expression of the gene encoding IL-1Rα (*Il1r1*) in BM-derived classically activated (M1) and alternatively activated (M2) macrophages, classified as such on the basis of differences in the expression of *Tnf*, *Nos2*, *Il12a*, *Arg1*, *Retnla* and *Chi313* mRNA[16] (**Supplementary Fig. 4b**). We found that M2 macrophages had higher expression of *Il1r1* mRNA than did M1 macrophages (**Fig. 6e**). We also found that subcutaneous injection of pertussis toxin, an inhibitor specific for inhibitory regulative G protein, almost completely abrogated the formation of DC clusters in response to hapten stimuli (**Fig. 6b**), which suggested that signaling through chemokines coupled to the inhibitory regulative G protein was required for the formation of DC clusters.

We next used microarray analysis to examine the effect of IL-1α on the expression of chemokine-encoding genes in M1 and M2 macrophages. Treatment with IL-1α did not enhance such expression in M1 macrophages, whereas it increased the expression of *Ccl5*, *Ccl17*, *Ccl22* and *Cxcl2* mRNA in M2 macrophages (**Supplementary Table 1**). Among those, *Cxcl2* mRNA expression was enhanced most prominently by treatment with IL-1α, a result we confirmed by real-time PCR analysis (**Fig. 6f**). Consistently, *Cxcl2* mRNA expression was much higher in DNFB-painted skin than in untreated skin (**Supplementary Fig. 5a**) and was not affected by neutrophil depletion with the 1A8 antibody to Ly6G (**Supplementary Fig. 5b**,**c**). In addition, IL-1α-treated dermal macrophages produced *Cxcl2* mRNA *in vitro* (**Supplementary Fig. 5d**). These results suggested that dermal macrophages, but not neutrophils, were the main source of CXCL2 during CHS. We also detected high expression of *Cxcr2* mRNA (which encodes the receptor for CXCL2) in DCs (**Supplementary Fig. 5e**); this prompted us to examine the role of CXCR2 in dDCs. The formation of DC clusters in response to DNFB was substantially reduced by intraperitoneal administration of the CXCR2 inhibitor SB265610 (ref. 17) (**Fig. 6g**). In addition, treatment with SB265610 during the elicitation of CHS with DNFB inhibited ear swelling (**Fig. 6h**) and IFN-γ production by skin T cells (**Fig. 6i**).

Together our results indicated that in the absence of effector T cells specific for a cognate antigen (i.e., in the sensitization phase of CHS), DC clustering was a transient event, and hapten-carrying DCs migrated into draining LNs to establish sensitization. On the other hand, in the presence of the antigen and antigen-specific effector or memory T cells, DC clustering was followed by accumulation of T cells (i.e., in the elicitation phase of CHS) (**Supplementary Fig. 6**). Thus, dermal macrophages were essential for initiating the formation of DC clusters through the production of CXCL2, and DC clustering had a role in the efficient activation of skin T cells.

DISCUSSION

Although the mechanistic events in the sensitization phase in cutaneous immunity have been studied thoroughly over 20 years[18,19], the types of immunological events that occur during the elicitation phases in the skin has remained unclear. Here we have described the antigen-dependent induction of DC–T cell clusters in the skin in a mouse model of CHS and showed that DC–effector T cell interactions in these clusters were required for the induction of efficient antigen-specific immune responses in the skin. We found that dDCs, but not epidermal LCs, were essential for the presentation of antigen to skin effector T cells and that they exhibited sustained association with effector T cells in an antigen- and LFA-1-dependent manner. IL-1α, not the inflammasome, initiated the formation of these perivascular DC clusters.

Epidermal contact with antigens triggers the release of IL-1 in the skin[15]. Published studies have shown that the epidermal keratinocytes constitute a major reservoir of IL-1α[6] and that mechanical stress applied to keratinocytes permits the release of large amounts of IL-1α even in the absence of cell death[20]. The cellular source of IL-1α in this process remains unclear. We found that IL-1α activated macrophages that subsequently attracted dDCs, mainly to areas around post-capillary venules, where effector T cells are known to transmigrate from the blood into the skin[21]. In the presence of the antigen and antigen-specific

effector T cells, DC clustering was followed by T cell accumulation. Therefore, we propose that these perivascular dDC clusters may provide antigen-presentation sites for efficient activation of effector T cells. This is suggested by the observations that CHS responses and intracutaneous T cell activation were attenuated substantially in the absence of these clusters, in conditions of macrophage depletion or inhibition of integrin function, IL-1R signaling[22,23] or CXCR2 signaling[24].

In contrast to antigen presentation in the skin, antigen presentation in other peripheral barrier tissues is relatively well understood. In submucosal areas, specific sentinel lymphoid structures (mucosa-associated lymphoid tissue (MALT)) serve as peripheral antigen-presentation sites[25], and lymphoid follicles are present in non-inflammatory bronchi (bronchus-associated lymphoid tissue (BALT)). These structures serve as antigen-presentation sites in nonlymphoid peripheral organs. By analogy, the concept of skin-associated lymphoid tissue (SALT) was proposed in the early 1980s, on the basis of findings that cells in the skin are able to capture, process and present antigens[26,27]. However, the role of cellular skin components as antigen-presentation sites has remained uncertain. Here we have identified an inducible structure formed by dermal macrophages, dDCs and effector T cells, which seemed to accumulate sequentially. Because formation of this structure was essential for efficient activation of effector T cells, these inducible leukocyte clusters may function as SALTs. Unlike leukocyte clusters in MALT, these leukocyte clusters were not found in the steady state but were induced during the development of an adaptive immune response. Therefore, these clusters might be better called 'inducible SALTs', similar to inducible BALTs in the lung[28]. In contrast to the cells present in inducible BALT, we did not identify naive T cells or B cells in SALT (data not shown), which suggested that the leukocyte clusters in the skin may be specialized for the activation of effector T cells but not for the activation of naive T cells. Our findings suggest that approaches for the selective inhibition of this structure may have novel therapeutic benefit in inflammatory disorders of the skin.

METHODS

Methods and any associated references are available in the online version of the paper.

Accession codes. GEO: microarray data, GSE53680.

Note: Any Supplementary Information and Source Data files are available in the online version of the paper.

ACKNOWLEDGMENTS

We thank H. Yagita (Juntendo University) for the KBA neutralizing antibody to LFA-1; P. Bergstresser and J. Cyster for critical reading of our manuscript. Supported by grants-in-aid for Scientific Research from the Ministry of Education, Culture, Sports, Science and Technology of Japan.

AUTHOR CONTRIBUTIONS

Y.N., G.E. and K.K. designed this study and wrote the manuscript; Y.N., G.E., S. Nakamizo, S.O., S.H., N.K., A.O., A.K., T. Honda and S. Nakajima performed the experiments and analyzed data; S.T. and Y.S. did experiments related to microarray analysis; K.J.I., H.T., H.Y., Y.I., M.K. and L.g.N. developed experimental reagents and gene-targeted mice; J.F. and E.G.-Y. did experiments related to immunohistochemistry of human samples; T.O., T. Hashimoto, Y.M. and K.K. directed the project and edited the manuscript; and all authors reviewed and discussed the manuscript.

COMPETING FINANCIAL INTERESTS

The authors declare no competing financial interests.

1. von Andrian, U.H. & Mempel, T.R. Homing and cellular traffic in lymph nodes. *Nat. Rev. Immunol.* **3**, 867–878 (2003).
2. Clark, R.A. *et al.* The vast majority of CLA+ T cells are resident in normal skin. *J. Immunol.* **176**, 4431–4439 (2006).
3. Wang, L. *et al.* Langerin expressing cells promote skin immune responses under defined conditions. *J. Immunol.* **180**, 4722–4727 (2008).
4. Tuckermann, J.P. *et al.* Macrophages and neutrophils are the targets for immune suppression by glucocorticoids in contact allergy. *J. Clin. Invest.* **117**, 1381–1390 (2007).
5. Sims, J.E. & Smith, D.E. The IL-1 family: regulators of immunity. *Nat. Rev. Immunol.* **10**, 89–102 (2010).
6. Murphy, J.E., Robert, C. & Kupper, T.S. Interleukin-1 and cutaneous inflammation: a crucial link between innate and acquired immunity. *J. Invest. Dermatol.* **114**, 602–608 (2000).
7. Nakae, S. *et al.* IL-1-induced tumor necrosis factor-α elicits inflammatory cell infiltration in the skin by inducing IFN-γ-inducible protein 10 in the elicitation phase of the contact hypersensitivity response. *Int. Immunol.* **15**, 251–260 (2003).
8. Thyssen, J.P., Linneberg, A., Menne, T., Nielsen, N.H. & Johansen, J.D. Contact allergy to allergens of the TRUE-test (panels 1 and 2) has decreased modestly in the general population. *Br. J. Dermatol.* **161**, 1124–1129 (2009).
9. Ng, L.G. *et al.* Migratory dermal dendritic cells act as rapid sensors of protozoan parasites. *Plos Pathog* **4**, e1000222 (2008).
10. Springer, T.A. & Dustin, M.L. Integrin inside-out signaling and the immunological synapse. *Curr. Opin. Cell Biol.* **24**, 107–115 (2012).
11. Egawa, G. *et al. In vivo* imaging of T-cell motility in the elicitation phase of contact hypersensitivity using two-photon microscopy. *J. Invest. Dermatol.* **131**, 977–979 (2011).
12. Miyawaki, S. *et al.* A new mutation, aly, that induces a generalized lack of lymph nodes accompanied by immunodeficiency in mice. *Eur. J. Immunol.* **24**, 429–434 (1994).
13. Sawaguchi, M. *et al.* Role of mast cells and basophils in IgE responses and in allergic airway hyperresponsiveness. *J. Immunol.* **188**, 1809–1818 (2012).
14. Otsuka, A. *et al.* Requirement of interaction between mast cells and skin dendritic cells to establish contact hypersensitivity. *PLoS ONE* **6**, e25538 (2011).
15. Enk, A.H. & Katz, S.I. Early molecular events in the induction phase of contact sensitivity. *Proc. Natl. Acad. Sci. USA* **89**, 1398–1402 (1992).
16. Weisser, S.B., McLarren, K.W., Kuroda, E. & Sly, L.M. Generation and characterization of murine alternatively activated macrophages. *Methods Mol. Biol.* **946**, 225–239 (2013).
17. Liao, L. *et al.* CXCR2 blockade reduces radical formation in hyperoxia-exposed newborn rat lung. *Pediatr. Res.* **60**, 299–303 (2006).
18. Honda, T., Egawa, G., Grabbe, S. & Kabashima, K. Update of immune events in the murine contact hypersensitivity model: toward the understanding of allergic contact dermatitis. *J. Invest. Dermatol.* **133**, 303–315 (2013).
19. Kaplan, D.H., Igyarto, B.Z. & Gaspari, A.A. Early immune events in the induction of allergic contact dermatitis. *Nat. Rev. Immunol.* **12**, 114–124 (2012).
20. Lee, R.T. *et al.* Mechanical deformation promotes secretion of IL-1 alpha and IL-1 receptor antagonist. *J. Immunol.* **159**, 5084–5088 (1997).
21. Sackstein, R., Falanga, V., Streilein, J.W. & Chin, Y.H. Lymphocyte adhesion to psoriatic dermal endothelium is mediated by a tissue-specific receptor/ligand interaction. *J. Invest. Dermatol.* **91**, 423–428 (1988).
22. Kish, D.D., Gorbachev, A.V. & Fairchild, R.L. IL-1 receptor signaling is required at multiple stages of sensitization and elicitation of the contact hypersensitivity response. *J. Immunol.* **188**, 1761–1771 (2012).
23. Kondo, S. *et al.* Interleukin-1 receptor antagonist suppresses contact hypersensitivity. *J. Invest. Dermatol.* **105**, 334–338 (1995).
24. Cattani, F. *et al.* The role of CXCR2 activity in the contact hypersensitivity response in mice. *Eur. Cytokine Netw.* **17**, 42–48 (2006).
25. Brandtzaeg, P., Kiyono, H., Pabst, R. & Russell, M.W. Terminology: nomenclature of mucosa-associated lymphoid tissue. *Mucosal Immunol.* **1**, 31–37 (2008).
26. Streilein, J.W. Skin-associated lymphoid tissues (SALT): origins and functions. *J. Invest. Dermatol.* **80** (suppl.), 12s–16s (1983).
27. Egawa, G. & Kabashima, K. Skin as a peripheral lymphoid organ: revisiting the concept of skin-associated lymphoid tissues. *J. Invest. Dermatol.* **131**, 2178–2185 (2011).
28. Moyron-Quiroz, J.E. *et al.* Role of inducible bronchus associated lymphoid tissue (iBALT) in respiratory immunity. *Nat. Med.* **10**, 927–934 (2004).

ONLINE METHODS

Mice. 8- to 12-week-old female C57BL/6 mice were used in this study. C57BL/6N mice were from SLC. Langerin-eGFP-DTR mice[29], CD11c-DTR mice[30], CD11c-YFP mice (that express CD11c tagged with YFP)[31], LysM-DTR mice[32], RAG-2-deficient mice[33], Mas-TRECK mice[13,14], Bas-TRECK mice[13,14], ALY/NscJcl- aly/aly mice[12], IL-1α/β-deficient mice[34], IL-1R1-deficient mice[35], NLRP3-deficient mice[36] and caspase-1/11-deficient mice[37] have been described. All experimental procedures were approved by the Institutional Animal Care and Use Committee of Kyoto University Graduate School of Medicine.

Human subjects. Biopsy samples of human skin were obtained from a nickel-reactive patch after 48 h after placement of nickel patch tests in patients with previously proven allergic contact dermatitis. A biopsy of petrolatum-occluded skin was also obtained as a control. Informed consent was obtained under protocols approved by the Institutional Review Board at the Icahn School of Medicine at Mount Sinai School Medical Center, and the Rockefeller University in New York.

Induction of CHS responses. Mice were sensitized on shaved abdominal skin with 25 μl 0.5% (wt/vol) DNFB (1-fluoro-2,4-dinitrofluorobenzene ; Nacalai Tesque) dissolved in acetone and olive oil (at a ratio of 4:1). Five days later, the ears were challenged with 20 μl 0.3% DNFB. For adoptive transfer, T cells were magnetically sorted, with an autoMACS (Miltenyi Biotec), from the draining LNs of sensitized mice and then were transferred intravenously (1×10^7 cells) into naive mice.

Depletion of cutaneous DC subsets, macrophages and neutrophils. For depletion of all cutaneous DC subsets (including LCs), 6-week-old Langerin-DTR mice were irradiated (two doses of 550 rads given 3 h apart) and were given transfer of 1×10^7 BM cells from CD11c-DTR mice. Eight weeks later, 2 μg DT (Sigma-Aldrich) was injected intraperitoneally. For selective depletion of LCs, irradiated Langerin-DTR mice were given transfer of BM cells from C57BL/6 mice, and 1 μg DT was injected. For selective depletion of dDCs, irradiated C57BL/6 mice were given transfer of BM cells from CD11c-DTR mice, and 2 μg DT was injected. For depletion of macrophages, irradiated C57BL/6 mice were given transfer of BM cells from LysM-DTR mice and 800 ng DT was injected. For depletion of neutrophils, anti-Ly6G (1A8; BioXCell) was administered to mice intravenously at a dose of 0.5 mg per mouse 24 h before experiments.

Time-lapse imaging of cutaneous DCs, macrophages and T cells. Cutaneous DCs were observed in CD11c-YFP mice. For labeling of cutaneous macrophages *in vivo*, 5 mg TRITC-dextran (Sigma-Aldrich) was injected intravenously and mice were allowed to 'rest' for 24 h. At that time, cutaneous macrophages became fluorescent because they had incorporated extravasated dextran. For labeling of skin-infiltrating T cells, T cells from DNFB-sensitized mice were labeled with CellTracker Orange (CMTMR (5-(and-6)-(((4-chloromethyl)benzoyl) amino)tetramethylrhodamine); Invitrogen) and were adoptively transferred into recipient mice. Keratinocytes and sebaceous glands were visualized by subcutaneous injection of isolectin B4 (Invitrogen) and BODIPY (Molecular Probes), respectively. Mice were positioned on a heating plate on the stage of a two-photon IX-81 microscope (Olympus) and their ear lobes were fixed beneath a cover slip with a single drop of immersion oil. Stacks of ten images, spaced 3 μm apart, were acquired at intervals of 1–7 min for up to 24 h. For calculation of T cell and DC velocities, movies were processed and analyzed with Imaris 7.2.1 software (Bitplane).

Histology and immunohistochemistry. For histological examination, tissues were fixed with 10% formalin in phosphate-buffered saline, then were embedded in paraffin. Sections with a thickness of 5 μm were prepared and then were stained with hematoxylin and eosin. For whole-mount staining, the ears were split into dorsal and ventral halves and were incubated for 30 min at 37 °C with 0.5 M ammonium thiocyanate. Then the dermal sheets were separated and fixed in acetone for 10 min at −20 °C. After treatment with Image-iT FX Signal Enhancer (Invitrogen), the sheets were incubated with antibody to mouse MHC class II (M5/114.15.2; eBioscience) followed by incubation with antibody to rat IgG conjugated to Alexa Fluor 488 (A-11006; Invitrogen) or Alexa Fluor 594 (A-11007; Invitrogen). The slides were mounted with a ProLong Antifade kit with the DNA-binding dye DAPI (4′6-diamidino-2-phenylindole; Molecular Probes) and were observed with a fluorescent microscope (BZ-900; KEYENCE). The number and size of DC clusters were evaluated in ten fields of 1 mm^2 per ear and were assigned scores according to the criteria in **Supplementary Figure 5a**.

Cell isolation and flow cytometry. For the isolation of skin lymphocytes, the split ears were incubated for 1 h at 37 °C in digestion buffer (RPMI medium supplemented with 2% FCS, 0.33 mg/ml of Liberase TL (Roche) and 0.05% DNase I (Sigma-Aldrich)). After that incubation, the tissues were disrupted by passage through a 70-μm cell strainer and stained with the appropriate antibodies (identified below). For analysis of intracellular cytokine production, cell suspensions were obtained in the presence of 10 μg/ml of brefeldin A (Sigma-Aldrich) and were fixed with Cytofix Buffer and permeabilized with Perm/Wash Buffer according to the manufacturer's protocol (BD Biosciences). Cells were stained with the following: antibody to mouse CD4 (GK1.5), anti-CD8 (53-6.7), anti-CD11b (M1/70), anti-CD11c (N418), anti-B220 (RA3-6B2), antibody to MHC class II (M5/114.15.2), anti-F4/80 (BM8), anti-IFN-γ (XMG1.2), anti-Gr1 (RB6-8c5) and 7-amino-actinomycin D (all from eBioscience); anti-mouse CD45 (30-F11) and anti-TCR-β (H57-597; both from BioLegend); and anti-CD16-CD32 (2.4G2; BD Biosciences). Flow cytometry was done with an LSR Fortessa (BD Biosciences) and data were analyzed with FlowJo software (TreeStarA).

Chemotaxis assays. Chemotaxis was assessed as described with some modifications[38]. The dermis of the ear skin was minced and then was digested for 30 min at 37 °C with 2 mg/ml collagenase type II (Worthington Biochemical) containing 1 mg/ml hyaluronidase (Sigma-Aldrich) and 100 μg/ml DNase I (Sigma-Aldrich). DDCs and macrophages were isolated with an autoMACS. Alternatively, BM-derived DCs and macrophages were prepared. 1×10^6 DCs were added to a Transwell insert with a pore size of 5 μm (Corning), and 5×10^5 macrophages were added to the lower wells, and the cells were incubated for 12 h at 37 °C. A known number of fluorescent reference beads (FlowCount fluorospheres; Beckman Coulter) were added to each sample to allow accurate quantification of cells that had migrated to the lower wells by flow cytometry.

Cell proliferation assay. Mice were sensitized with 25 μl 0.5% DNFB or 7% trinitrochlorobenzene (Chemical Industry). Five days later, T cells were magnetically separated from the draining LNs of each group of mice and were labeled with CellTrace Violet according to the manufacturer's protocol (Invitrogen). 1×10^6 T cells were adoptively transferred into naive mice, and the ears of the recipient mice were challenged with 20 μl of 0.5% DNFB. 24 h later, ears were collected and analyzed by flow cytometry.

***In vitro* differentiation of DCs and M1 and M2 macrophages from BM cells.** BM cells from the tibias and fibulas were plated at a density of 5×10^6 cells per 10-cm dish on day 0. For DC differentiation, cells were cultured at 37 °C in 5% CO_2 in cRPMI medium (RPMI medium supplemented with 1% L-glutamine, 1% HEPES, 0.1% 2-mercaptoethanol and 10% FBS) containing 10 ng/ml granulocyte-macrophage colony-stimulating factor (Peprotech). For macrophage differentiation, BM cells were cultured in cRPMI medium containing 10 ng/ml macrophage colony-stimulating factor (Peprotech). The medium was replaced on days 3 and 6 and cells were harvested on day 9. For the induction of M1 macrophages or M2 macrophages, cells were stimulated for 48 h with IFN-γ (10 ng/ml; R&D Systems) or with IL-4 (20 ng/ml; R&D Systems), respectively.

***In vitro* IL-1α-stimulation assay of dermal macrophages.** Dermal macrophages were separated from mice deficient in IL-1α and IL-1β[34] to avoid preactivation during cell preparations. Split ears were treated for 30 min at 37 °C with 0.25% trypsin and EDTA for removal of the epidermis, then were minced and then incubated with collagenase as described above. $CD11b^+$ cells were separated by magnetic-activated cell sorting, and 2×10^5 cells per well in 96-well plates were incubated for 24 h with or without 10 ng/ml IL-1α (R&D Systems).

doi:10.1038/ni.2992

Blocking assay. For the LFA-1-blocking assay, mice were given intravenous injection of 100 μg KBA (neutralizing antibody to LFA-1; a gift from H. Yagita) 12–14 h after challenge with 20 μl 0.5% DNFB. For blockade of IL-1R, mice were given subcutaneous injection of 10 μg recombinant mouse IL-1ra (PROSPEC) 5 h before challenge. For blockade of CXCR2, mice were given intraperitoneal treatment with 50 μg CXCR2 inhibitor[17] (SB265610; Tocris Bioscience) 6 h before and at the time of painting of the skin with hapten.

Quantitative PCR analysis. Total RNA was isolated with an RNeasy Mini kit (Qiagen, Hilden, Germany). cDNA was synthesized with a PrimeScript RT reagent kit and random hexamers according to the manufacturer's protocol (TaKaRa). A LightCycler 480 and LightCycler SYBR Green I Master mix were used according to the manufacturer's protocol (Roche) for quantitative PCR (primer sequences, **Supplementary Table 2**). The expression of each gene was normalized to that of the control gene *Gapdh*.

Microarray analysis. Total RNA was isolated with an RNeasy Mini Kit according to the manufacturer's protocol (Qiagen). An amplified sense-strand DNA product was synthesized with the Ambion WT Expression Kit (Life Technologies), was fragmented and labeled by the WT Terminal Labeling and Controls Kit (Affymetrix) and was hybridized to a Mouse Gene 1.0 ST Array (Affymetrix). We used the robust multiarray average algorithm for log transformation ($\log_2$) and normalization of the GeneChip data.

General experimental design and statistical analysis. For animal experiments, a sample size of three to five mice per group was used on the basis of past experience in generating statistical significance. Mice were randomly assigned to study groups and no specific randomization or blinding protocol was used. Sample or mouse identity was not masked for any of these studies. Prism software (GraphPad) was used for statistical analyses. Normal distribution was assumed a priori for all samples. Unless indicated otherwise, an unpaired parametric *t*-test was used for comparison of data sets. In cases in which the data-point distribution was not Gaussian, a nonparametric *t*-test was also applied. *P* values of less than 0.05 were considered significant.

29. Kissenpfennig, A. *et al.* Dynamics and function of Langerhans cells *in vivo*: dermal dendritic cells colonize lymph node areas distinct from slower migrating Langerhans cells. *Immunity* **22**, 643–654 (2005).
30. Jung, S. *et al. In vivo* depletion of CD11c$^+$ dendritic cells abrogates priming of CD8$^+$ T cells by exogenous cell-associated antigens. *Immunity* **17**, 211–220 (2002).
31. Lindquist, R.L. *et al.* Visualizing dendritic cell networks *in vivo*. *Nat. Immunol.* **5**, 1243–1250 (2004).
32. Miyake, Y. *et al.* Protective role of macrophages in noninflammatory lung injury caused by selective ablation of alveolar epithelial type II Cells. *J. Immunol.* **178**, 5001–5009 (2007).
33. Hao, Z. & Rajewsky, K. Homeostasis of peripheral B cells in the absence of B cell influx from the bone marrow. *J. Exp. Med.* **194**, 1151–1164 (2001).
34. Horai, R. *et al.* Production of mice deficient in genes for interleukin (IL)-1α, IL-1β, IL-1α/β, and IL-1 receptor antagonist shows that IL-1β is crucial in turpentine-induced fever development and glucocorticoid secretion. *J. Exp. Med.* **187**, 1463–1475 (1998).
35. Coban, C. *et al.* Immunogenicity of whole-parasite vaccines against *Plasmodium falciparum* involves malarial hemozoin and host TLR9. *Cell Host Microbe* **7**, 50–61 (2010).
36. Martinon, F., Petrilli, V., Mayor, A., Tardivel, A. & Tschopp, J. Gout-associated uric acid crystals activate the NALP3 inflammasome. *Nature* **440**, 237–241 (2006).
37. Koedel, U. *et al.* Role of caspase-1 in experimental pneumococcal meningitis: evidence from pharmacologic caspase inhibition and caspase-1-deficient mice. *Ann. Neurol.* **51**, 319–329 (2002).
38. Tomura, M. *et al.* Activated regulatory T cells are the major T cell type emigrating from the skin during a cutaneous immune response in mice. *J. Clin. Invest.* **120**, 883–893 (2010).

COMMENTARY

See related article on pg 1255

Cytokine Regulation during Epidermal Differentiation and Barrier Formation

Atsunari Tsuchisaka[1], Minao Furumura[1] and Takashi Hashimoto[1]

The role of structural components and cell adhesion molecules in the epidermis has not been fully studied in terms of the pathophysiology of atopic dermatitis (AD). In this issue, Omori-Miyake *et al.* (2014) report that IL-4 and IL-13, which are Th2 cytokines, downregulate the expression of keratins and desmosomal cadherins in a STAT6-dependent manner, leading to keratinocyte fragility in the face of mechanical stress. Th2 cytokine–induced instability of the epidermis may be considered to be one of the pathogenic mechanisms that have roles in AD.

Journal of Investigative Dermatology (2014) **134,** 1194–1196; doi:10.1038/jid.2014.15

The epidermis maintains its integrity and stability primarily through the expression of cellular structural components and adhesion molecules (Simpson *et al.*, 2011; Omori-Miyake *et al.*, 2014). To achieve terminal differentiation, the epidermis undergoes keratinization, whereas its keratinocytes move from the stratum basale (basal layer) to the stratum spinosum (spinal layer), stratum granulosum (granular layer), and, as a final product, the stratum corneum (cornified layer; Figure 1, left panel; Simpson *et al.*, 2011).

The expression patterns of epidermal keratins, profilaggrin/filaggrin, and desmosomal cadherins, i.e., desmogleins 1–4 (Dsg1–Dsg4) and desmocollins 1–3 (Dsc1–Dsc3), have been studied extensively (Simpson *et al.*, 2011; Figure 1, left panel). Importantly, keratin 5 and keratin 14 are expressed at the basal layer, whereas keratin 1 and keratin 10 are expressed in suprabasal layers. Profilaggrin is expressed in the upper epidermis and it is processed into filaggrin through proteolysis. With respect to desmosomal cadherins, Dsc1, Dsg1, and Dsg4 are expressed strongly in the upper epidermis, whereas Dsg2, Dsg3, Dsc2, and Dsc3 are expressed strongly in the lower epidermis. Finally, corneodesmosin, a component of corneodesmosome, is expressed in the upper epidermis.

The component proteins of the tight junction have been shown to be expressed in the epidermis by immunofluorescence analyses (Tunggal *et al.*, 2005) and they are now thought to have important roles in skin barrier development. Tight junction proteins were detected mainly at the boundary between the granular and cornified layers; i.e., occludin and ZO-1 are found in the granular layer, whereas claudin 1 is expressed in the whole living epidermis (Figure 1, left panel).

Abnormalities in these structural components and cell adhesion molecules have been studied mainly in the hereditary bullous and keratinizing diseases and in the autoimmune bullous diseases. Thus, it is now known that gene mutations in keratin 5 or keratin 14 cause epidermolysis bullosa hereditaria simplex, whereas mutations in keratin 1 or keratin 10 cause epidermolytic ichthyosis (formerly, bullous congenital ichthyosiform erythroderma). In addition, reduced expression of filaggrin, by virtue of gene mutations, is now known to cause ichthyosis vulgaris and to facilitate the development of atopic dermatitis (AD).

In contrast, cutaneous and mucosal bullous lesions in the various types of pemphigus are caused by pathogenic autoantibodies directed against specific desmosomal cadherins, i.e., Dsg1, Dsg3, and Dsc1–Dsc3 (Hashimoto *et al.*, 2012). These autoantibodies tend to produce histopathological changes in the epidermis, precisely where the targeted desmosomal cadherins are expressed. Thus, pemphigus foliaceus and pemphigus vulgaris show acantholytic changes in the upper and lower portions of the epidermis, respectively, where the target antigens, Dsg1 and Dsg3, respectively, are expressed. In addition, subcorneal pustular dermatosis type IgA pemphigus shows an accumulation of neutrophils in the uppermost epidermis, where the target antigen, Dsc1, is expressed.

Terminal differentiation of the epidermis is achieved by several orchestrated processes, namely, lipid production and extrusion, formation of a filaggrin/keratin network in the cytoplasm, formation and disruption of desmosomes, and formation of cornified envelopes, as well as the formation of tight junctions in the upper epidermis (Figure 1, right panel). In the formation of the cornified envelope, several precursor proteins are expressed and bound to each other by activated transglutaminase 1. Various desmosomal cadherins and corneodesmosin function in keratinocyte cell adhesion, and they are degraded by proteolysis before desquamation. Epidermal keratins and filaggrin form the keratin network in the cornified layer. Lipids are synthesized and extrude outside corneocytes; tight junction proteins are also expressed to form the junctions. Coordination of these processes is essential to the maintenance of a stable epidermis.

Several earlier studies have examined the role of cytokines in the regulation of expression of structural components and cell adhesion molecules, and on the development of the epidermal barrier during differentiation to a cornified layer (Gutowska-Owsiak and Ogg, 2013; Hänel *et al.*, 2013; Figure 1, right panel).

These studies have suggested that most allergic inflammation-related cytokines affect the expression of epidermal

[1]*Department of Dermatology, Kurume University School of Medicine, and Kurume University Institute of Cutaneous Cell Biology, Kurume, Japan*

Correspondence: Takashi Hashimoto, Department of Dermatology, Kurume University School of Medicine, and Kurume University Institute of Cutaneous Cell Biology, 67 Asahimachi, Kurume, Fukuoka 830-0011, Japan. E-mail: hashimot@med.kurume-u.ac.jp

Received 12 December 2013; accepted 14 December 2013